

A study of the electronic states of pyrimidine by electron energy loss spectroscopy

Ireneusz Linert, Mariusz Zubek*

*Department of Physics of Electronic Phenomena, Gdańsk University of Technology,
80-233 Gdańsk, Poland*

Abstract

The electron energy loss spectra were measured in pyrimidine at the constant electron residual energy varied from 15 meV to 10 eV and in the scattering angle range 0-180°. The spectra were analysed applying an iteration fitting procedure to resolve the energy loss bands corresponding to excitation of the electronic states of pyrimidine. The vertical excitation energies of the singlet states of pyrimidine and of a number of the triplet states were determined. The presently observed triplet states were tentatively assigned.

* Corresponding author.

E-mail address: mazub@mif.pg.gda.pl

1. Introduction

The electron energy loss spectroscopy is a powerful technique in the studies of the excited states of polyatomic molecules, providing important complementary spectroscopic data to that obtained from photoabsorption spectra. It was experimentally confirmed that performing the combined variable scattering angle and the residual electron energy measurements differentiation between and identification of the optically-allowed and -forbidden transitions could be achieved [1, 2]. Here, at low scattering angles and a high residual electron energy (> 10 eV) the excitation of the optically-allowed states dominates the energy loss spectra, while at the lower residual electron energy (< 3 eV) and large scattering angles the relative intensity of the optically-forbidden transitions increase. In particular, the scattering at 180° should be governed by the electron exchange interaction which favours singlet-triplet excitation. Moreover, the spin- and symmetry-forbidden transitions usually dominate in the near-threshold spectra measured at low residual electron energy. It has also been pointed out on the ground of group theoretical considerations that in the symmetry-forbidden transitions the differential excitation cross section at 0° and 180° (electron axial scattering) should be zero for diatomic molecules and relatively low for polyatomic molecules [3].

The present work aims to provide new data on the excited states of pyrimidine by measuring and analyzing the electron energy loss spectra obtained at the constant residual electron energy varied from 15 meV to 10 eV and at the selected scattering angles from 0° to 180° . Pyrimidine (1,3-diazine), $C_4H_4N_2$, belongs to azabenzenes, a group of molecules that are isoelectronic with benzene (C_6H_6). It has a planar ring geometry incorporating two nitrogen heteroatoms at positions 1 and 3 and belongs to the C_{2v} point group in the electronic ground state. In comparison with benzene, replacement of two C–H groups with nitrogen atoms in the



benzene ring shifts the energy levels to higher values and gives rise to new transitions due to excitation of nitrogen lone pair electrons from the non-bonding (n_N) orbitals. The relatively simple pyrimidine molecule is often considered as a molecular model of the purine nucleic acids (thymine, cytosine) and thus have recently gained an increased interest in the studies of interaction and damage induced by ionizing radiation in the biological matter [4].

The electronic configuration of the outermost molecular valence orbitals of the \tilde{X}^1A_1 ground state of pyrimidine may be written as $\dots(1a_2)^2(11a_1)^2(2b_1)^2(7b_2)^2$ [5,6], while the lowest unoccupied molecular orbitals are $(2a_2)(3b_1)(12a_1)(4b_1)$ [6,7]. The $11a_1$ and $7b_2$ orbitals have been identified as the non-bonding (n_N) orbitals, while the $1a_2$, $2b_1$ and the unoccupied $2a_2$ and $3b_1$ orbitals as having π character [5]. Consequently, in the low energy range the pyrimidine excitation spectrum will contain bands corresponding to the $n_N\pi^*$ and $\pi\pi^*$ states of the A_2 , B_1 and A_1 , B_2 symmetries, respectively. However, it is worth noting, as demonstrated by the calculations [5], that some of the excited states of pyrimidine have to be described by taking into account the configuration interaction and vibronic coupling.

The excited electronic states of pyrimidine in the 3.5–11 eV energy range have been assigned in the photoabsorption measurements [5,6,8,10,11]. Some earlier works have been critically reviewed in [12]. The photoabsorption spectrum of pyrimidine contains three distinct broad bands at 5.2, 6.7 and 7.5 eV, which are accompanied by two lower intensity bands at 4.2 and 8.9 eV. These bands were assigned to the 1B_2 , 1A_1 , 1A_1 and 1B_2 , 1B_1 singlet states, respectively. Some of the bands show superimposed vibrational structure of the excited Rydberg states. There is much less spectroscopic data on the triplet states and symmetry-forbidden transitions in pyrimidine. The lowest lying 3B_1 triplet state of pyrimidine has been firmly located by observing laser-induced phosphorescence bands, which have an origin at 3.538 eV [13,14]. To observe the triplet states at higher energies the near-threshold electron



energy loss spectra were measured using the trapped electron technique [9,10]. The rather weak features in the excitation spectrum of [10] were assigned with an aid of the multi-reference configuration interaction calculations, but were reassigned in [11]. The electron energy loss spectra have been recently obtained for the impact energies of 15–50 eV and the scattering angle range 10–90° in the measurements of the differential cross sections [15,16]. Six excitation bands of unresolved valence singlet and triplet states have been recorded in the energy range from 3–10 eV. High impact energy (150 eV) energy loss spectrum was also reported previously [17]. Apart from the above gas phase studies, the electronic excitation of pyrimidine have been equally investigated for the three-layer films deposited on solid argon in the low incident energy range 2–12 eV [18]. In this studies, the main features below 7 eV in the energy loss spectra were ascribed to the triplet states.

A number of theoretical calculations on the electronic states of pyrimidine, which applied *ab initio* and density functional approaches have been also performed [5,10,11,19-24]. These works deliver rather more results on the spectroscopy of the singlet than the triplet states. A fair consistency has been achieved for the singlet states between different theoretical approaches and the experiment.

Experimental details

The electron energy loss spectra in pyrimidine were measured employing electron spectrometer that has been described in detail in our previous publication [25]. It consists of a source of energy-selected electrons, a capillary to produce the target gas beam and a scattered electron analyzer that can be rotated around the axis of the gas beam. It also incorporates a magnetic angle changer [26] to extend the scattering angle range from 90° to 180°. The electron analyzer was equipped with an extracting electrode [27] to implement a penetrating electrostatic field technique [28] for the measurements of the threshold energy loss spectra.

The electron spectrometer is also furnished with a magnetic field deflector placed between the exit of the hemispherical selector in the electron analyzer and the electron channel multiplier [27]. It was used to estimate the possible contribution of low kinetic energy negative ions into the threshold electron spectra. Such contributions, if present, were below 5% of the scattered electron intensity.

All spectra recorded were measured in the mode of the constant residual electron energy E_R . At E_R energies between 2 and 10 eV the scattered electrons were collected at a fixed scattering angle. In the threshold mode of operation of the analyzer ($E_R < 0.15$ eV), electrons were collected from a larger solid angle (up to 4π) of the scattering region. The energy loss spectra were measured with an energy resolution of 60–80 meV (FWHM). The electron energy loss scale in the non-threshold mode was determined against the elastic scattering peak with an uncertainty of ± 5 meV. In the threshold mode, the electron energy loss was calibrated against the position of the 2^1S excitation peak in helium to within ± 5 meV, by measuring the threshold spectra in mixture with pyrimidine. In this mode, the E_R energy was estimated from the intensity ratio of the 2^1S to 2^3S threshold peaks [29].

The scattering angle Θ was calibrated against known positions of minima in the elastic electron scattering in argon with an uncertainty of $\pm 1.5^\circ$. However, in the measurements with the magnetic angle changer, the angular uncertainty was higher, for example $\pm 3^\circ$ at 180° . This was caused by the energy dependence on the deflection of the incident electron beam in the magnetic field. To minimize this effect, the energy loss spectra at 180° were measured in the shorter energy ranges and the obtained spectra were combined into a final spectrum. To aid the angular calibration, the electron trajectories in the magnetic field were simulated using CPO computer program [30].

The liquid pyrimidine with a stated purity of 98% was purchased from Sigma-Aldrich. The sample was kept in a stainless steel container heated to approximately 40° C. The pyrimidine vapour was introduced into the spectrometer by a gas line kept at 50° C, while the apparatus was at 60° C. The pyrimidine in the container was degassed several times under low pressure.

2. Results

The electron energy loss spectra measured in pyrimidine at $E_R=10$ eV, $\Theta=10^\circ$ and $E_R=3$ eV, $\Theta=180^\circ$ are presented in Figure 1a and b, respectively. The (a) spectrum displaying energy loss bands at 4.2, 5.2, 6.7 and 7.6 eV resembles well that of the VUV photoabsorption measurements [6]. Although its relative band intensities differ from those of the VUV spectrum, both spectra demonstrate the highest intensity band at 7.6 eV. The shape of the present spectrum is also in accord with that measured previously in [16] and [17] at electron energy of 50 and 150 eV, respectively. The (b) spectrum obtained at lower E_R energy and backward scattering shows increased intensities of the energy loss bands at 4.2 and 5.2 eV together with a slightly lower width of the 7.6 eV band. A detailed comparison of the (a) and (b) spectra reveals differences in the positions of the maxima in the 5.2 and 6.7 eV bands. The shift of the maxima and the variation of the shapes and widths of the 5.2 eV energy loss band are clearly demonstrated in Figure 2, which compares two threshold spectra measured at $E_R=15$ and 140 meV with an energy loss spectrum of $E_R=10$ eV and $\Theta=30^\circ$. For example, the maximum in the $E_R=140$ meV spectrum appears 60 meV below that of the $E_R=10$ eV spectrum. The increased widths and variation of the shapes of the bands in the threshold spectra undoubtedly indicate the excitation of several pyrimidine states in this energy region. Some of these states, observed in the threshold spectra may correspond to the triplet states.

Similarly, it is seen that the second maximum in the $E_R=140$ meV threshold spectrum is placed 84 meV below that in the $E_R=10$ eV spectrum.

To resolve the excitation bands in the measured energy loss spectra, they were fitted with a set of Gaussian profiles. The initial set containing an adequate number of profiles was determined in the following manner. It started by considering the spectra measured at $E_R=10$ eV and low scattering angles (see Figure 1a). As these spectra approximate the VUV photoabsorption results, the band profiles were placed at the energies of 4.2, 5.2, 6.7 and 7.6 eV, the positions of the observed singlet states [6]. The widths (FWHM) of the bands were estimated from the photoabsorption spectra, for example, the width of the 5.2 eV band was taken to be 0.4 eV [6]. Next, the scattered intensities observed between the first two singlet bands were approximated by a single profile placed at 4.7, while that between second and third singlet bands by two profiles placed at 5.7 and 6.0 eV. The $E_R=140$ meV threshold spectrum (Figure 2) indicates clearly an energy loss band at about 4.4 eV. To account for energy shifts and variation of the shape of the 5.2 eV peak in the threshold spectra (Figure 2), two Gaussian profiles were introduced, one below (4.9 eV) and one above (5.4 eV) the singlet band at 5.2 eV. The 6.7 eV peak was approximated by two closely spaced bands of similar widths. Further, the 7.6 eV energy loss peak was fitted with two Gaussians of much different intensities to justify for its asymmetry on the low energy slope, which is also seen in the photoabsorption spectrum [6]. Finally, the $E_R=3$ eV, $\Theta=180^\circ$ (Figure 1) and the $E_R=140$ meV (Figure 2) spectra show weak shoulders at about 3.9 eV, which corresponds to the lowest excited state of pyrimidine.

The assembled set of fifteen introductory bands, reproducing the features observed in the energy loss spectra was optimized to fit the experimental spectra. In the optimization strategy, to reduce the number of simultaneously correlated Gaussians (fitting their energies and

widths), single fits were carried out in shorter but overlapping energy regions (1-2 eV wide) in the area of the 5.2, 6.7 and 7.6 eV singlet bands. These single fits were repeated in the iteration mode and were stopped when the overall fits to the energy loss spectra gave satisfactory agreement. It is of note, that the positions and widths of the excitation bands obtained in this manner from fifteen individual complete spectra were consistent to better than ± 30 and ± 50 meV, respectively. Figure 3 presents results of the fitting and shows positions of the resolved excitation bands and the final fits to the three energy loss spectra of pyrimidine.

3. Discussion

The obtained vertical excitation energies of the electronic states of pyrimidine are listed in Table 1 and are compared with results of the VUV absorption, electron impact and theoretical works. These energies represent the average values of those obtained from fitting the energy loss spectra. Their uncertainties are lower than ± 35 meV. As seen in Table 1 some of the present energies are in excellent agreement with those obtained in the photoabsorption measurements [6,8]. Thus, they indicate excitation bands of the singlet states. The assignment of the singlet states in Table 1 follows determined in [5]. Table 1 displays also energies of the excitation bands, which were not observed in the absorption and may correspond to the electron impact excitation of the optically forbidden states. The tentative assignment of these states is given in Table 1.

The lowest energy band at 3.85 eV, detected only in the threshold and near-threshold ($E_R \leq 3$ eV) spectra, is assigned to excitation of the 1^3B_1 triplet state. The band energy agrees well with the origin of the band observed in the laser-induced phosphorescence at 3.538 eV [13,14] and with the results of the theoretical calculations of Fisher et al. [11]. The energy of the next excitation band seen in the energy loss spectra of 4.18 eV coincides with that obtained from the absorption measurements by Ferreira da Silva et al. [6]. This band has been



earlier assigned to the singlet 1^1B_1 state [12]. Its excitation is obviously seen in our spectra obtained at the higher E_R energies and low scattering angles favouring optically allowed transitions (see Figure 1a). The spectra measured at lower E_R and higher scattering angles (see Figure 1b) show, however, significantly increased intensity of this band with respect, for example, to that of the 7.6 eV singlet band. This observation suggests excitation of a triplet state, a second state contributing to the intensity of the 4.18 eV band. Indeed, the extensive theoretical studies of [11] predict the 1^3A_2 state at 4.19 and 4.24 eV in the density functional TD-B3LYP and the ab initio CASPT2 studies, respectively. We assign the second state contributing to the 4.18 eV band to the 1^3A_2 symmetry and this supports the earlier reassignment of threshold excitation results of Palmer et al. [10] carried out in [11]. The 4.42 eV excitation band in our spectra is attributed to the 1^3A_1 state on the ground of comparison with the theoretical calculations which locate this state at 4.35-4.45 eV [5,11,19]. In the threshold and near-threshold spectra this band has a substantial intensity against the singlet bands what further corroborates the above assignment.

Bolovinos et al. [8], in their absorption studies reported a band system near 4.6 eV, which they ascribed, relying on results of the theoretical calculations, to the 1^1A_2 state. The excitation transition to the 1^1A_2 state is symmetry forbidden but it could become allowed via vibronic coupling to the 1^1B_2 state [8]. Although, the 1^1A_2 transition has not been detected recently by Ferreira da Silva et al. [6], we do resolve an excitation band in our energy loss spectra at 4.69 eV, which may well correspond to the 1^1A_2 state of [8]. Moreover, the obtained excitation energy is in accord with the results of several recent calculations [19,20,23,24]. The next excitation band in the spectra observed at 4.93 eV is assigned to the 1^3B_2 state, the last remaining triplet state of the lowest energy $n_N\pi^*$ and $\pi\pi^*$ transitions. It broadens the 5.2 eV energy loss peak in the threshold spectra (see Figure 3a) and contributes

to the intensity between the first and second singlet bands in the near-threshold spectra (see Figure 3c). In this assignment the 1^3B_2 state would appear 0.25 eV below the 1^1B_2 singlet state, which we find at 5.18 eV. The energy of 0.25 eV gives a reasonable value for the singlet-triplet splitting in the B_2 symmetry [11,19]. Our energy of 5.18 eV for the 1^1B_2 state is in excellent agreement with the energies obtained in the photoabsorption measurements [5,6,8] (Table 1). However, the E_R energy dependence of the relative intensity of the 5.18 eV peak (against those of the singlet states), in particular its high intensity in spectra of Figure 1b and 3b, allows to suggest the contribution of a triplet state to the 5.18 eV peak. The extensive theoretical calculations have foreseen the 2^3A_1 state between 5.13 and 5.27 eV [11,19] and we assign tentatively the second state to this symmetry.

The two excitation bands at 5.43 and 5.67 eV in the present spectra are ascribed to the triplet and singlet states of the $2A_2$ symmetry, respectively. Both bands contribute with higher intensities to the threshold and near-threshold spectra (see Figure 3) but are rather weak in the $E_R=10$ eV spectra. Callis [31] in his two-photon absorption studies in pyrimidine dissolved in hexane revealed a 1^1A_1 state at 5.6 eV, which was next identified in the near-threshold electron energy loss spectrum of [10]. The 0.24 eV energy difference between the 2^1A_2 singlet and the 2^3A_2 triplet states is an acceptable singlet-triplet splitting. The next two bands at 6.02 and 6.69 eV correlate very well with the positions of the two singlet bands observed in the photoabsorption measurements [5,6,8]. The first band was assigned consistently to the 2^1B_1 state [5,6,8], whereas the second band was reassigned recently by Stener et al. [5] to the 1^1A_1 state. They were aided by results of their calculations and this assignment is in agreement with some earlier theoretical works [19,23,24]. Previously, the second band was attributed to the 2^1A_1 state, the second state of the 1^1A_1 symmetry [6,11]. The photoabsorption spectra show additionally vibrational structure superimposed on the 1^1A_1 band [5,6], which was related to

excitation of the 3s Rydberg state. The last band below 7 eV seen in our spectra at 6.56 eV appears clearly only in the threshold and near-threshold spectra (see Figure 3) allowing for its assignment to a triplet state. We tentatively ascribe it to the 2^3B_2 state following calculations of Fisher et al. [11].

The most intense peak in the pyrimidine energy loss spectra at 7.6 eV is fitted with a low intensity band at 7.27 eV responsible for a shoulder on the low-energy slope of the main peak and with the main band having maximum at 7.58 eV. In accordance with Stener et al. [5] we associate these two bands with excitation of the 2^1A_1 and 3^1B_2 singlet states, respectively. The photoabsorption results show vibrational structure on the slopes of the peak due to the excitation of the 3p Rydberg states [5,6]. In the 8-9.5 eV region a band at 8.2 eV is found in our spectra (see insets in Figure 3), which may correspond to excitation of the Rydberg states converging to the $7b_2^{-1} \tilde{X}^2B_2$ ionization limit at 9.8 eV (the energy of the peak of the photoelectron band) [32].

4. Conclusions

The electron energy loss spectra were measured in pyrimidine at the constant electron residual energy varied from 15 meV (threshold spectra) to 10 eV and in the scattering angle range 0-180°. The spectra were analysed applying an iteration fitting procedure to resolve the energy loss bands corresponding to excitation of the electronic states of pyrimidine. This approach permitted to distinguish the excitation bands of the singlet states. The obtained vertical excitation energies of these states of pyrimidine are in excellent accord with the results of the absorption studies. Using characteristics of the electron impact excitation, also allowed to distinguish a number of the triplet states and determine their vertical excitation energies. The triplet states were tentatively assigned, comparing the present energies with the results of the extensive theoretical calculations. Nonetheless, it should be pointed out that a

rather simplified picture of the individual bands resolved in the energy loss spectra, assuming one-electron excitation, may be more complex because of the configuration interaction and overlapping of the excitation bands of closely lying electronic states of pyrimidine. The identification of the triplet states in the present work contributing to the first and second energy loss bands supports conclusions of Jones et al [16] drawn out from the angular behaviour of their differential cross sections measured in the 15-50 eV energy range.

References

- [1] S. Trajmar, J.K. Rice, A. Kuppermann, *Adv. Chem. Phys.* 18 (1970) 15.
- [2] M. Allan, *J. Electron. Spectrosc. Rel. Phenom.* 48 (1989) 219.
- [3] W.A. Goddard III, D.L. Huestis, D.C. Cartwright, S. Trajmar, *Chem. Phys. Lett.* 11 (1971) 329.
- [4] R. Colmenares, A.G. Sanz, M.C. Fuss, F. Blanco, G. Garcia, *App. Rad. Isotop.* 83 (2014) 91.
- [5] M. Stener, P. Decleva, D.M.P. Holland, D.A. Shaw, *J. Phys. B* 44 (2011) 075203.
- [6] F. Ferreira da Silva, D. Almeida, G. Martins, A.R. Milosavljevic, B.P. Marinkovic, S.V. Hoffmann, N.J. Mason, Y. Nunes, G. Garcia, P. Limão-Vieira, *Phys. Chem. Chem. Phys.* 12 (2010) 6717.
- [7] A. Modelli, P. Bolognesi, L. Avaldi, *J. Phys. Chem. A* 115 (2011) 10775.
- [8] A. Bolovinos, P. Tsekeris, J. Philis, E. Pantos, G. Andritsopoulos, *J. Mol. Spectrosc.* 103

(1984) 240.

[9] M. N. Pisanias, L. G. Christophorou, J.G. Carter, D.L. McCorkle, *J. Chem. Phys.* 58

(1973) 2110.

[10] M.H. Palmer, I.C. Walker, M.F. Guest, A. Hopkirk, *Chem. Phys.* 147 (1990) 19.

[11] G. Fischer, Z.-L. Cai, J.R. Reimers, P. Wormell, *J. Phys. Chem. A* 107 (2003) 3093.

[12] K.K. Innes, I.G. Ross, W.R. Moomaw, *J. Mol. Spectrosc.* 132 (1988) 492.

[13] T. Takemura, K. Uchida, M. Fujita, Y. Shindo, N. Suzuki, H. Baba, *Chem. Phys. Lett.* 73

(1980) 12.

[14] C. Ottinger, A.F. Vilesov, T. Winkler, *Chem. Phys. Lett.* 208 (1993) 299.

[15] D.B. Jones, S.M. Bellm, P. Limão-Vieira, M.J. Brunger, *Chem. Phys. Lett.* 535 (2012)

30.

[16] D.B. Jones, S.M. Bellm, F. Blanco, M. Fuss, G. García, P. Limão-Vieira, M.J. Brunger,

J. Chem. Phys. 137 (2012) 074304.

[17] L. Åsbrink, C. Fridh, B.Ö. Jonsson, E. Lindholm, *Int. J. Mass Spectrom. Ion Phys.* 8

(1972) 215.

[18] P.L. Levesque, M. Michaud, L. Sanche, *J. Chem. Phys.* 122 (2005) 094701.

[19] Y.J. Li, J. Wan, X. Xu, *J. Comput. Chem.* 28 (2007) 1658.

[20] M. Biczysko, J. Bloino, G. Brancato, I. Cacelli, C. Cappelli, A. Ferretti, A. Lami, S.



Monti, A. Pedone, G. Prampolini, C. Puzzarini, F. Santoro, F. Trani, and G. Villani,

Theor. Chem. Acc. 131 (2012) 1201.

[21] Z. Masin, J.D. Gorfinkiel, D.B. Jones, S.M. Bellm, M.J. Brunger, J. Chem. Phys. 136

(2012) 144310.

[22] P.-Å. Malmqvist, B.O. Roos, M.P. Fülcher, A.P. Rendell, Chem. Phys. 162 (1991) 359.

[23] M. Nooijen, Spectrochim. Acta part A, 55 (1999) 539.

[24] J.E. Del Bene, J.D. Watts, R.J. Bartlett, J. Chem. Phys. 106 (1997) 6051.

[25] I. Linert, M. Zubek, J. Phys. B 39 (2006) 4087.

[26] I. Linert, G.C. King, M. Zubek, J. Electr. Spectrosc. Rel. Phenom. 134 (2004) 1.

[27] M. Zubek, M. Dampc, I. Linert, T. Neumann, J. Chem. Phys. 135 (2011) 134317.

[28] S. Cvejanovic, F. H. Read, J. Phys. B 7 (1974) 1180.

[29] R.K. Nesbet, Phys. Rev. A 12 (1975) 444.

[30] See <http://www.electronoptics.com> for information about the CPO programs.

[31] P.R. Callis, J. Chem. Phys. 75 (1981) 5640.

[32] D.M.P. Holland, A.W. Potts, L. Karlsson, M. Stener, P. Decleva, Chem. Phys. 390
(2011) 25.

Figure captions

Figure 1

Electron energy loss spectra measured in pyrimidine for the constant residual energy E_R and the scattering angle Θ : (a) 10 eV and 10° , (b) 3 eV and 180° .

Figure 2

Electron energy loss spectra measured in pyrimidine for the constant residual energy $E_R=15$ and 140 meV in the threshold mode and for $E_R=10$ eV and the scattering angle $\Theta=30^\circ$. Also shown are (full lines) final fits to the experimental spectra.

Figure 3

Electron energy loss spectra measured in pyrimidine for the constant residual energy E_R and the scattering angle Θ : (a) 140 meV in the threshold mode, (b) 3 eV and 180° , (c) 10 eV and 30° . Also shown are (full lines) excitation bands fitted to the experimental spectra and their final fits.

TABLE 1. Vertical excitation energies (in electronvolts) of the electronic states of pyrimidine.

Present work	Experiment				Calculations				Assignment	
	VUV [5]	VUV [6]	VUV [8]	EEL [10]	TD-B3LYP [11]	CASPT2 [11]	SAC-CI [19]	EOM-CC [24]		
4.18		4.183	3.851 ^a		4.31	4.26	4.32	4.24	7b ₂ →2a ₂	1 ¹ B ₁
4.69	4.638 ^b	-	4.62	≈4.7	4.55	4.49	4.74	4.74	7b ₂ →3b ₁	1 ¹ A ₂
5.18	5.022 ^a	5.22	5.12		5.87	5.17	5.29	5.01	2b ₁ →2a ₂	1 ¹ B ₂
5.67				≈5.7	5.75		5.98	5.84	11a ₁ →2a ₂	2 ¹ A ₂
6.02	6.0 ^c	~6.0	6.05		5.94	6.03	6.35	6.11	11a ₁ →3b ₁	2 ¹ B ₁
6.69	6.7 ^c	6.69 ^d	6.7				6.86	6.57	2b ₁ →3b ₁	1 ¹ A ₁
7.27					6.69	7.10			1a ₂ →2a ₂	2 ¹ A ₁
7.58	7.5 ^c	7.478 ^c	7.57							3 ¹ B ₂
3.85				3.6	3.73	3.81	4.11		7b ₂ →2a ₂	1 ³ B ₁
4.18				≈4.5	4.19	4.24	4.71		7b ₂ →3b ₁	1 ³ A ₂
4.42					4.11	4.35	4.39		2b ₁ →3b ₁	1 ³ A ₁
4.93				5.05	4.76	4.83	4.81		2b ₁ →2a ₂	1 ³ B ₂
5.18					5.25	5.13	5.27		1a ₂ →2a ₂	2 ³ A ₁
5.43					5.13	5.39	5.81		11a ₁ →2a ₂	2 ³ A ₂
6.56					5.98	6.51	6.35		1a ₂ →3b ₁	2 ³ B ₂

a – band origin

b – member of vibrational progression

c – energy estimated from published spectra

d – assigned to 2¹A₁

e – assigned to 3¹A₁ + 2¹B₂

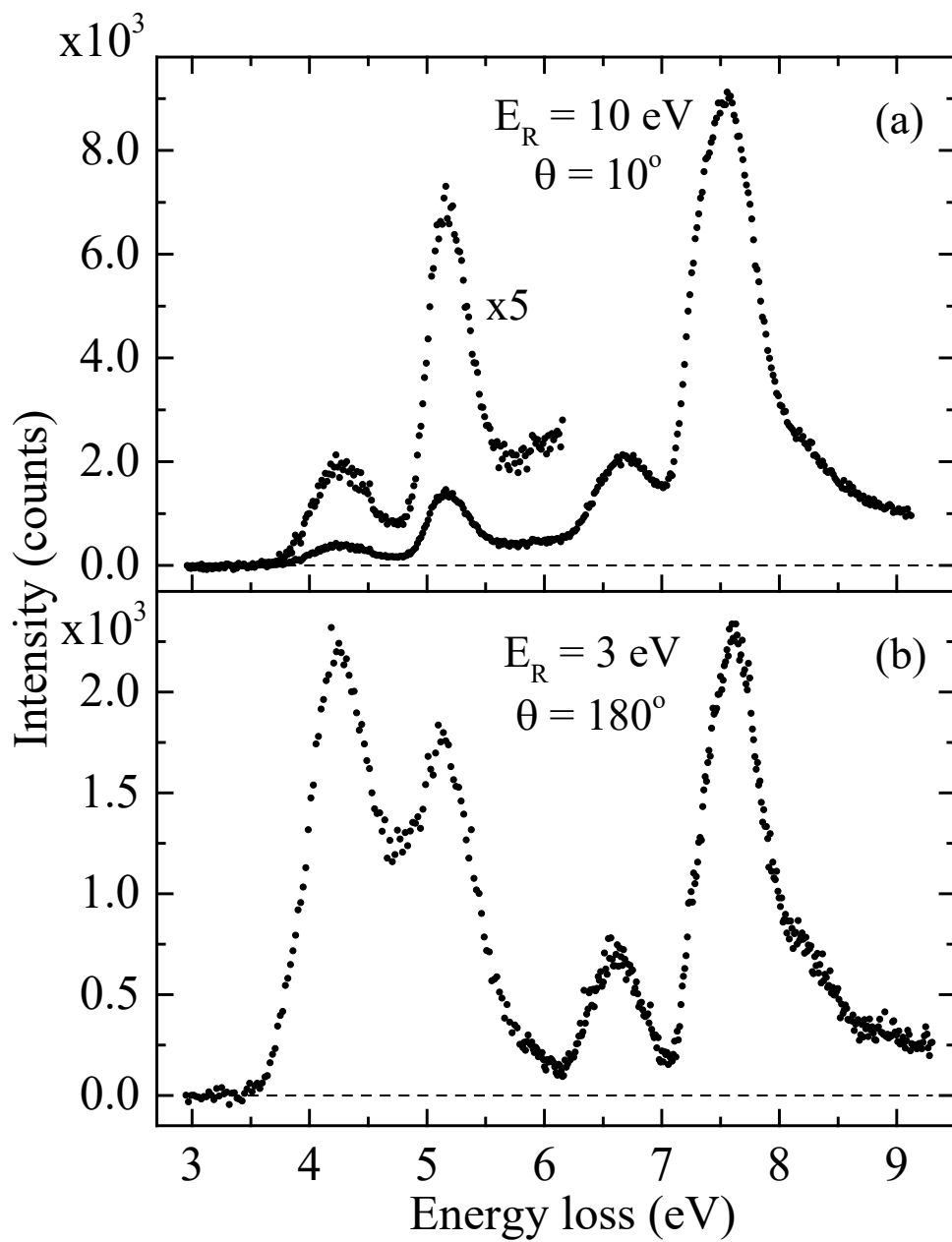


Figure 1



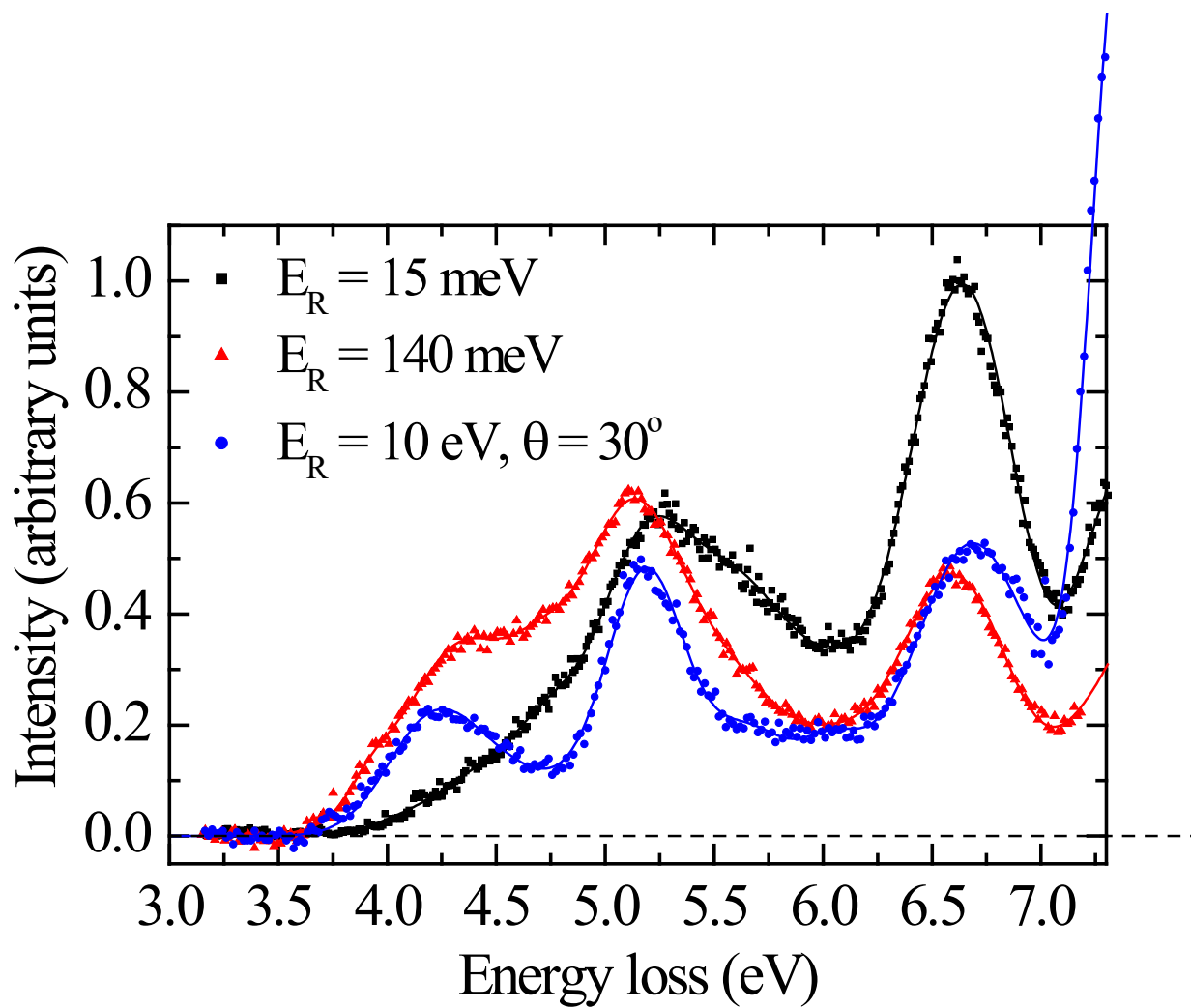


Figure 2

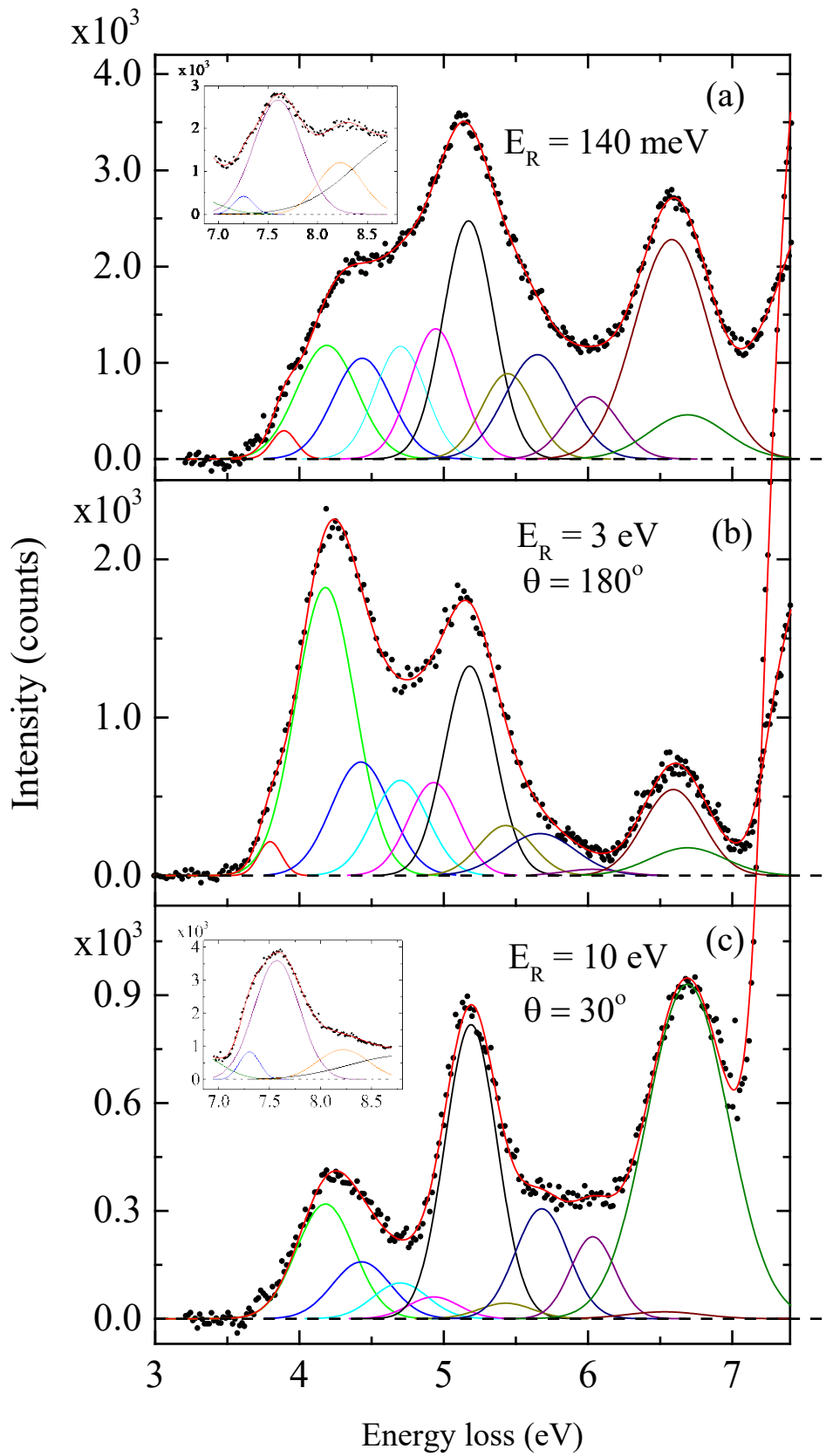


Figure 3